The dynamics of hydrogen bonds and proton transfer in zeolites - joint vistas from solid-state NMR and quantum chemistry

Topics in Catalysis 9 (1999) 163–180

The dynamics of hydrogen bonds and proton transfer in zeolites – joint vistas from solid-state NMR and quantum chemistry

Hubert Koller [a,*], Günter Engelhardt [b] and Rutger A. van Santen [c]

[a] *Institute of Physical Chemistry, University of Münster, 48149 Münster, Germany*
[b] *Institute of Chemical Technology I, University of Stuttgart, 70550 Stuttgart, Germany*
[c] *Schuit Institute of Catalysis, Eindhoven University of Technology, 5600 MB Eindhoven, The Netherlands*

The different aspects of zeolite Brønsted acid sites are reviewed from the perspective of solid-state NMR spectroscopy and quantum-chemical calculations. The strength of the combined use of these two methods is demonstrated. Special emphasis is dedicated to the structure and dynamics of hydrogen-bonded complexes of zeolites with H_2O and CH_3OH.

Keywords: zeolites, solid-state NMR, quantum-chemical calculations, acidity, hydrogen bonds, dynamics

1. Introduction

1.1. General

Zeolites are open framework structures that are built up by corner-sharing $AlO_{4/2}^{-}$ and $SiO_{4/2}$ tetrahedra. Charge balance is provided by extra-framework cations. The H-forms of these types of materials are acidic, and they have achieved a tremendous significance as catalysts [1–3]. The catalytic properties such as reactivity and product selectivity are determined by the nature of the zeolite and by selected chemical pre-treatments. The characterization of Brønsted acidity has been a major topic in zeolite science. Nowadays it is acknowledged that zeolites are not superacids, as for instance pointed out in a recent review by Haw et al. [4]. Some of the most intriguing challenges in the science of zeolite catalysts are the structural characterization of the acid site, the understanding of the bonding, and the study of proton transfer equilibria in the presence of reacting molecules. Most of the investigations thus far were aimed at pinpointing the detailed structure in a frozen state of the system. The implications of the dynamics in the study of proton transfer processes in zeolites are far more difficult to understand due to a lack of systematic dynamic models or insights that can be extracted from experimental data. This circumstance is mainly caused by the limitations of the available methods, especially if they are applied in a stand-alone manner. The dynamic time scale of solid-state NMR spectroscopy is for instance too slow, making only the dynamically averaged state accessible for this technique, and high-level quantum-chemical ab initio calculations are to date very time-consuming to study the full pathway of a dynamic process in zeolite catalysts. Here we offer some general strategies and principles that can be used to understand proton transfer and dynamic phenomena in zeolites, if these methods are used in tandem. The paper will be driven by a cooperative use of solid-state NMR spectroscopy and quantum-chemical calculations.

There has been much controversy lately about the question as to whether or not water and methanol molecules get protonated in zeolites in the ground state. A large amount of work is being published in this field. We believe that a compilation of fundamental aspects regarding bonding and dynamics, and their theoretical and spectroscopic characterization will be useful for future discussions. Thus, the primary goal of this paper is to offer some strategies and new perspectives which represent a state-of-the-art in the understanding of the zeolitic acid site and its reactivity. We pursue a purely molecular approach with the intent to emphasize the mechanistic picture of a zeolite catalyst. Therefore, the characterization of the structural and dynamical details is a main goal, and the distinct local bonding properties and their change in dynamic processes in catalytically relevant model systems were the prominent motivation for writing this overview.

The paper is organized in the following way. At first, a brief introduction will be given about the functional properties of acidic zeolite catalysts. This section is divided into two parts: we will start with a discussion of the local acid site and then the influence of the zeolite as a porous host matrix will be addressed. Computational chemistry has become a valuable tool for the study of catalytic processes. Therefore, a brief overview will be dedicated to the quantum-chemical methods that are currently applied to the interactions of molecules in zeolites (section 2). The main part of this paper (section 3) is dominated by solid-state NMR spectroscopy as a tool to investigate the interaction between H_2O and CH_3OH with zeolitic acid sites. The combination of NMR spectroscopy with quantum-chemical calculations will be a key issue, and special emphasis is devoted to the structure of hydrogen bonds and their dynamics.

* To whom correspondence should be addressed.

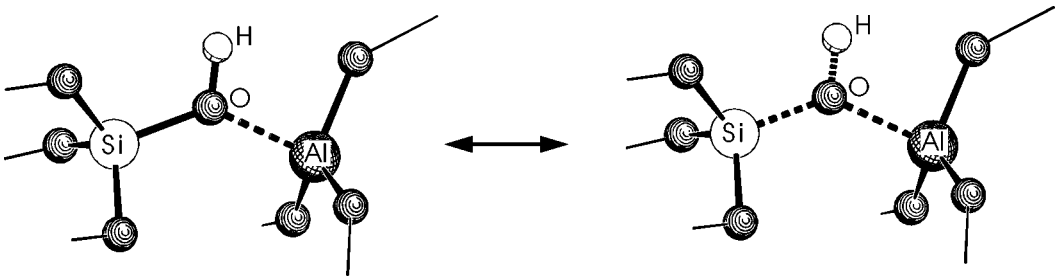

Scheme 1.

1.2. The acid site

A Brønsted acid site is formed by a proton attached to a bridging oxygen atom between two tetrahedral atoms: silicon and aluminum. This structure constitutes a formally three-coordinated oxygen atom [2,5,6]. The two models in scheme 1 illustrate some principles of the bonding situation at the acid site, and the broken lines stand for the weakening of the bonds with respect to the unprotonated zeolite. The acid proton perturbs the local structure of the zeolite by weakening the adjacent Si–O and Al–O bonds. The model on the left-hand side of scheme 1 illustrates that the Al–O bond experiences a larger change in bond strength than the adjacent Si–O bond upon protonation/deprotonation.

The deprotonation energy of such an acid site is ca. 1200 kJ/mol, as resulting from quantum-chemical calculations, while an isolated terminal SiOH group is significantly more stable towards deprotonation (∼1400 kJ/mol) [7–10]. This difference can be rationalized if the Brønsted site of a zeolite is regarded as a SiOH group which is promoted by the interaction of the oxygen atom with the neighbored Lewis acidic aluminum in the framework (electron-pair-accepting site) [11–13].

The local bond properties of the Brønsted hydroxyl group have been extensively studied by infrared and ^{1}H NMR spectroscopies [14–26]. Much less attention has been dedicated to the promoting function of the Al–O bond, which is displayed as a broken line in scheme 1. Some recent results from ^{27}Al NMR spectroscopy will be shown later that address this issue (section 3.4). It will be demonstrated that new perspectives regarding the dynamics of methanol are arising from these considerations.

1.3. The zeolite matrix and adsorption complexes

The overall properties of H-zeolites are also influenced by their global structural properties, in addition to the local structure. For instance the number density and the distribution of catalytically active sites are of great importance, and the pore sizes in the zeolite and their dimensionality have an influence on the catalytic performance. Since proton transfer reactions are always acid–base reactions, more factors are important, e.g., the accessibility of the Brønsted proton, the proton affinity of the base, and the adsorption energies of the protonated and unprotonated probe molecules in the particular zeolite void. Some of the basic principles of the activity of the Brønsted sites emerging from structural or bonding properties of zeolites are collected in figure 1 which shows two principal axes as guidelines. The upper part pronounces the intrinsic properties of a bare zeolite, and the lower part focusses on the interaction of a zeolite loaded with a probe molecule. Cooperative effects of adsorbed probe molecules (not considered in figure 1) can also play a role if the loading is higher than one molecule per acid site, or when the distances between active sites are small. In addition, it has been shown that coadsorbed solvent molecules can promote proton transfer [27]. The second, horizontal axis in figure 1 divides the properties into local versus global (matrix) contributions.

The typical working field of spectroscopic techniques is on the left-hand side of figure 1. The contributions from computational chemistry are from both sides, the left and the right. The cluster approach is usually selected to study local properties by ab initio or density functional methods which allow for sophisticated calculations of subtle details of local structure and bonding. If matrix effects have to be considered, then the cluster can be embedded in force fields, representing the zeolite matrix [28]. Alternatively, periodic ab initio calculations are becoming possible, especially due to advances with the method introduced by Car and Parinello [29]. The developments of faster computers and better quantum-chemical methods are ongoing, promising further improvements in the future.

The complexity of the problem in figure 1 clearly increases from the upper left to the lower right corner. The upper left of figure 1 represents the aforementioned local bonding properties in the zeolite model shown in scheme 1. This was the starting point of spectroscopic techniques to the study of the Brønsted site.

It has been suggested that local structural constraints are caused by the zeolite framework, that is to say some rigidity of the zeolite exists due to crystalline structure [5] (upper right of figure 1). This framework strain prevents the local structure of the acid site (Si–(OH)–Al) to fully relax from the geometry or original volume of a Si–O–Si bridge [30,31]. While the relaxation that can be achieved is local, and it is accomplished within a few bonds in the framework, the framework strain can be of long-range origin. If this geometric strain from the crystalline zeolite is imposed on the local structure, then differences in proton activities can be explained for different zeolites. Recent improvements in quantum-chemical embedding methods suggest that the

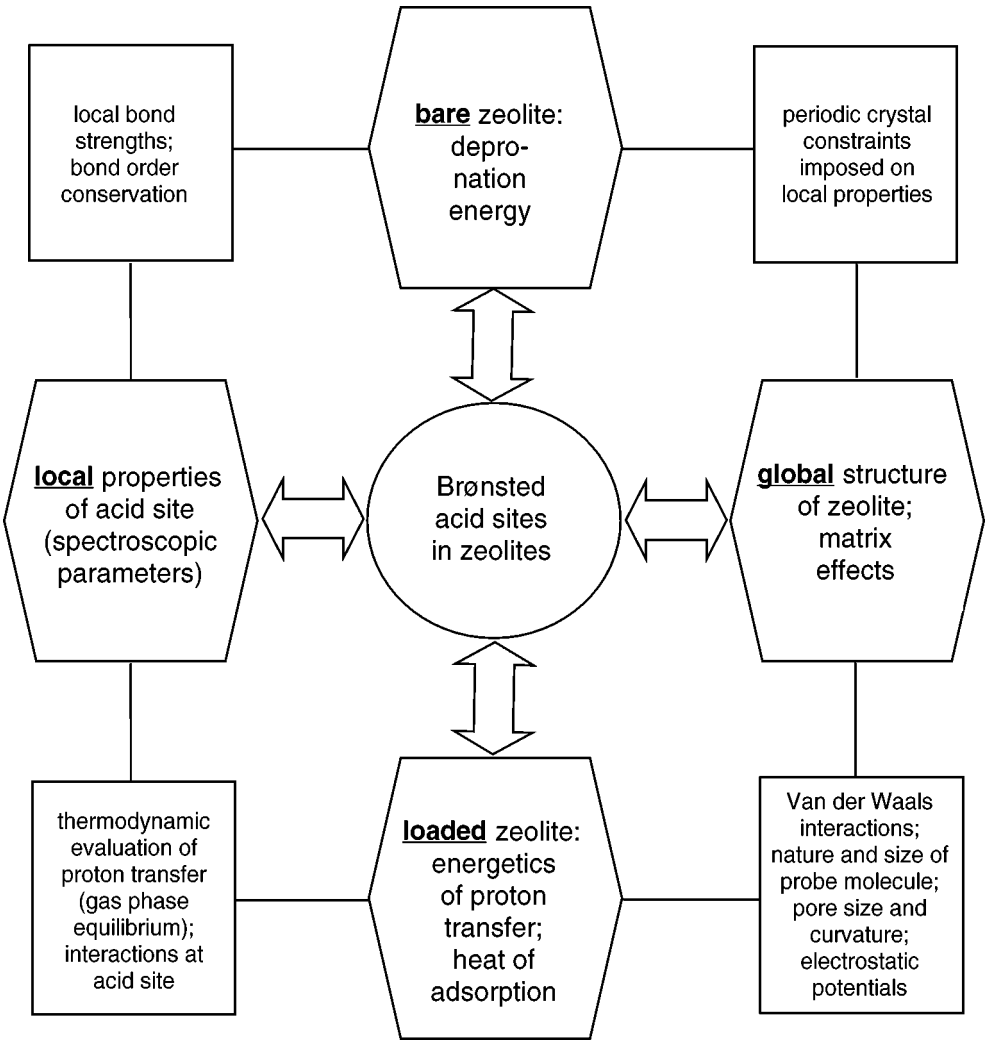

Figure 1. Structural principles and properties of the zeolite acid site.

long-range interactions play an important role in the evaluation of deprotonation energies in zeolites [8].

An interesting solid-state NMR experiment that adds some evidence has been reported by Sarv et al. [32]. The work of these authors was devoted to proton mobilities in bare zeolites. The dehydrated zeolites H-ZSM-5, H-mordenite, and H-Y have been studied by ^{1}H MAS NMR spectroscopy at various temperatures up to 660 K. The motivation of these experiments was the determination of activation parameters for proton mobility based on a method which was originally introduced and recently reviewed by Hunger [33]. The activation energies for jumps of the Brønsted protons to neighboring oxygen atoms were found to be 45, 54, and 61 kJ/mol for HZSM-5, H-mordenite, and HY, respectively. However, the mechanism of that particular motion is as yet unknown which leaves some open question regarding the meaning of the given numbers when they are compared with model calculations. Early quantum-chemical cluster calculations by Sauer resulted in an activation energy of ca. 52 kJ/mol for such a proton jump process [7] which is in the range of the experimental observations by Sarv et al. The experimental differences for the three zeolites indicate that there is indeed a measurable difference in proton mobility, depending on the zeolite matrix. The early cluster calculation did not consider matrix effects, and, therefore, does not explain the subtle differences for the three zeolites, but nevertheless, it obviously predicts rather well the dominating local energetic contribution. A very recent quantum-chemical study using embedding techniques of Sauer et al. reveals higher values between 75 and 110 kJ/mol for the activation energy of proton jumps in H-chabasite and H-faujasite [34]. By the embedding method, differences have been predicted for different proton sitings and different zeolite structures. Much lower experimental activation energies of 17–20 kJ/mol have been reported by Baba et al. for H-ZSM-5 [35], using the same method as Sarv et al. [32].

These and other results add to the upper part of figure 1 and they are important for understanding the dynamic properties of the Brønsted protons. However, in lieu of studying the intrinsic properties of a Brønsted site, e.g., by its individual deprotonation energy, infrared or NMR spectra, it appears to be more relevant for catalytic properties to investigate the interactions between the solid acid and adsorbed

probe molecules (lower part of figure 1). The interaction of the Brønsted proton with a basic probe molecule weakens the zeolitic O–H bond, causing increased bond strengths between the oxygen atom to its neighbored tetrahedral centers, silicon and aluminum. These cooperative changes in bond strengths counterpoise each other in such a way that the sum of bond orders of one particular atom remains constant. This rule is referred to as the bond order conservation principle [13]. This rule is a quantum-chemical analogue of the bond valence concept based on the early ideas of Pauling [36].

The study of the Brønsted site by means of the adsorption of probe molecules will be discussed in more detail here. To this end, we choose the probe molecules H_2O and CH_3OH as the model system. Discerning proton transfer in the adsorption complex is sometimes difficult to prove, as shall be demonstrated by the two selected examples. These subjects are of interest, mainly because they reveal our level of understanding of solid-state acidity. Activation of CH_3OH by zeolitic protons is the first step in the conversion of methanol to gasoline [37]. The question as to whether or not proton transfer to these probe molecules occurs in the ground state is still a matter of ongoing debate. The fact that the answer is not trivial is underlined by a paper by Smith et al. [38], who studied the adsorption of H_2O in H-SAPO-34 by neutron diffraction and infrared spectroscopy. An H_3O^+ hydroxonium ion is formed in the eight-ring channel of the zeolite and a hydrogen-bonded water molecule is located on a Brønsted proton of a six-ring of the H-SAPO-34 structure. That means that both cases exist within one structure, depending on the location of the acid site. Ab initio calculations on model clusters suggest that the energy of the ion pair structure is only about 10 kJ/mol higher than the neutral complex [39]. This situation might change easily due to matrix effects, making the proton transfer process sensitive to small changes in the global environment or the presence of additional water molecules [40], a recognition which strengthens the importance of the right part in figure 1. Another interesting result has been obtained from a picosecond laser infrared experiment, where a transient spectrum is obtained that indicates hydrogen-bonded H_2O adsorbed in H-mordenite [41].

Since with NH_3 protonation undoubtedly occurs, both possibilities, proton transfer and neutral adsorption of H_2O and CH_3OH, must be deemed possible, and it may even depend on the particular system which is the right answer. These questions raise considerable experimental and computational challenges. On the other hand, this means that H_2O and CH_3OH are suitable probe molecules in that they probe the borderline of proton reactivity which means that they are potentially able to discriminate between reactive and unreactive sites.

2. Insights from theory

Quantum-chemical methods require a rigorous treatment of hydrogen bonds and other weak interactions in order to yield a reliable description of the zeolitic acid site with adsorbed probe molecules. Therefore, semiempirical methods have found only limited use in this field. Ab initio calculations have an inherent restriction of the size of the system that can be studied, because of the large computational demands. Until recently, these studies have been applied only to relatively small clusters in the gas phase which resulted in important insights into the local properties of the zeolite acid site (left side of figure 1) [13,45]. The disadvantage of this strategy is that the constraints of the zeolite framework relaxation is not sufficiently treated and long-range potentials are neglected. Periodic ab initio calculations are not applicable for most zeolites due to the large unit cells, making the system too large for these methods. An alternative are density functional calculations with plane wave basis sets [42–44]. The latest development is the embedding of a quantum mechanically treated cluster model in a periodic potential [28].

The main contribution of computational chemistry is the recognition that in zeolites protonated species are often only transition states rather than local minima structures as sketched in figure 2. Proton transfer requires cleavage of a strong O–H bond ($E_b \approx 1300$ kJ/mol) and charge sep-

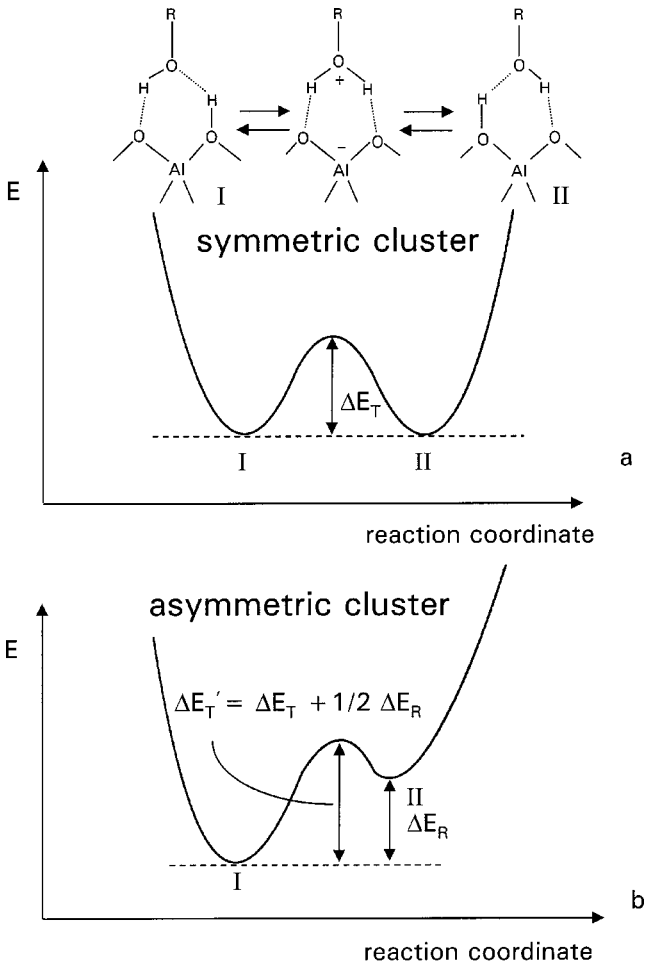

Figure 2. Potential energy diagrams of symmetric and asymmetric proton exchange reactions.

aration. The zeolite has a low dielectric constant ($\varepsilon \approx 2$), so that the stabilizing interaction between the negatively charged zeolite wall and the protonated species plays a dominant role.

For this reason carbonium ions as well as carbenium ions in zeolites are nearly always highly activated transition states, and their counterparts are covalently bonded alkoxy species. For molecules such as CH_3OH or H_2O this implies that protonated methoxonium or hydronium ions are preferably transition states rather than ground states.

A major issue in computational chemistry is the use of the cluster assumption. Elsewhere this has been extensively discussed [13,45]. Here we like to emphasize an important difference between embedded and non-embedded clusters: whereas small clusters are usually symmetric, with equivalent oxygen atoms, it has been pointed out by Kramer et al. [46] that oxygen atoms surroundings are not equivalent. Their deprotonation energies can differ in energy by 10–80 kJ/mol. Hence, the potential energy diagram should be better represented by figure 2(b), rather than figure 2(a). $\Delta E'_{\mathrm{T}}$ is the activation energy when oxygen atoms are non-equivalent, ΔE_{T} is the activation energy with equivalent oxygen atoms, and ΔE_{R} is the difference in energy between I and II [47]. The inequivalence of oxygen atoms may be the main reason for the difference between the actually measured proton exchange rate and the computed one based on cluster potential energy diagrams such as figure 2(a).

Infrared spectroscopy has significantly contributed to the issue of hydrogen bonding versus proton transfer. When proton transfer does not occur, the interaction between a basic adsorbate (such as acetonitrile) and the zeolitic proton weakens the zeolite proton bond and enhances its dipole moment. The Pauli repulsive interaction between base electron occupied orbitals and OH orbitals is released by polarization of the OH bond, the polarization being stronger the more electropositive the zeolite OH environment. The infrared spectrum shows a downwards shifted and more intense band, but also a significant broadening of the band occurs, because of a coupling between OH stretching modes and the external base molecule – proton modes.

When the base strongly weakens the OH frequency, as happens with H_2O, CH_3OH or CH_3CN, the strongly broadened OH stretching band becomes split into a double or triple structure due to Fermi resonance with overtones of the upward shifted zeolite OH bending modes [48]. The occurrence of these "A,B,C patterns" for chemisorbed H_3O and CH_3OH provides direct proof of hydrogen bonding of the interacting bases.

3. Solid-state NMR spectroscopy

One of the major advantages of NMR spectroscopy is its element selectivity. One has the choice to select a local probe in the structure (NMR active nucleus) and the experimental conditions (NMR techniques) according to special needs. Thus, the potential of solid-state NMR methods to help unravel the puzzle of proton transfer in zeolites depends on the particular nuclear properties (here: ^{1}H, ^{2}H, ^{27}Al).

Solid-state NMR spectroscopy has been used to study intermediates in the methanol-to-gasoline (MTG) process, and novel in-situ techniques have been applied [49–52]. In this paper we will confine ourselves to the first elementary step of the catalytic process: the adsorption structure at the active site. Solid-state NMR measurements on zeolites loaded with probe molecules other than H_2O or CH_3OH have been carried out by several groups (see, for example, [22,23,53–72]).

We start with an overview of the structural information on O–H$\cdots$O hydrogen bonds attainable by proton chemical shifts. Isotropic chemical shifts in NMR spectra and their structural information are influenced by dynamic processes. If the exchanging species have different chemical shifts, then their weighted average is observed in NMR spectra. The second part introduces the additional information on hydrogen bonds that can be achieved by ^{2}H NMR spectroscopy and the insights by this method into dynamic processes will be outlined. The use of anisotropic properties of nuclear spins and their power in providing dynamic information will be addressed. Among all molecular sieves with different tetrahedral framework elements, incorporation of aluminum creates the highest catalytic activity of Brønsted protons [7,10,73–75]. In principle it should be possible to characterize the function of Lewis acidity of framework Al (cf. scheme 1) by ^{27}Al NMR spectroscopy, which will be further explained with special emphasis on dynamic aspects.

3.1. Proton chemical shifts and hydrogen bonds in model structures

3.1.1. Hydrogen bonds and proton chemical shifts in various structures

The ^{1}H chemical shift of the protons in O–H$\cdots$O hydrogen bonds in solids can vary over a wide range, as already shown in 1980 by the classical paper of Berglund and Vaughan [76]. These authors have studied a variety of solids including organic and inorganic hydrates and carboxylic acids, and a correlation between the ^{1}H chemical shifts and the O$\cdots$O distances in O–H$\cdots$O hydrogen bonds has been established. Rohlfing et al. [77] have carried out a theoretical study on hydrogen-bonded dimers of RCOOH or ROH. The proton chemical shift tensor in these clusters is nearly axially symmetric which means that only two spatial tensor components, the components parallel and perpendicular to the principal shielding direction, have to be considered. The direction of the parallel chemical shift component, $\delta_{\|}$, is almost, though in general not exactly, parallel to the O–H bond. It was found that the chemical shift perpendicular to this bond, $\delta_{\perp}$, correlates well with the O$\cdots$O distance, but $\delta_{\|}$ does not. Thus, the observed correlation between the isotropic chemical shift and

the O···O distance, $d_{O\cdots O}$, is dominated by the perpendicular contribution to the proton shielding. These authors also found that the change in proton chemical shift tensors upon hydrogen-bond formation is mainly influenced by the nature of the proton acceptor. We will come back to this important finding later.

The work of Berglund and Vaughan was further extended by other groups [78–83]. Jeffrey and Yeon have found a correlation between the proton chemical shift and the H···O hydrogen-bond distance [79]. Since δ_H correlates with $d_{O\cdots O}$, the well-known dependence of the covalent d_{O-H} distance on $d_{O\cdots O}$ [76] leads to the conclusion that δ_H must be also a function of d_{O-H}. Such a direct correlation between the covalent O–H distance and the ^{1}H chemical shift in hydrogen bonds has been theoretically predicted by Ditchfield using quantum-chemical calculations of the chemical shift in the water dimer [84].

Sternberg and Brunner [83] have collected proton chemical shift data of compounds where the hydrogen-bond structures are well determined on the basis of neutron diffraction data. Here, these data are utilized for illustrating (figure 3, open circles) the correlation between δ_H and the O–H (lower part) or O···H (upper part) distances in O–H···O hydrogen bonds. The data from [83] for $CaHPO_4$ (monetite) and $Ca(OH)_2$ were not included in figure 3 due to structural uncertainty about the crystallographic space group (inversion symmetry or not) [85] or motional effects [86], respectively.

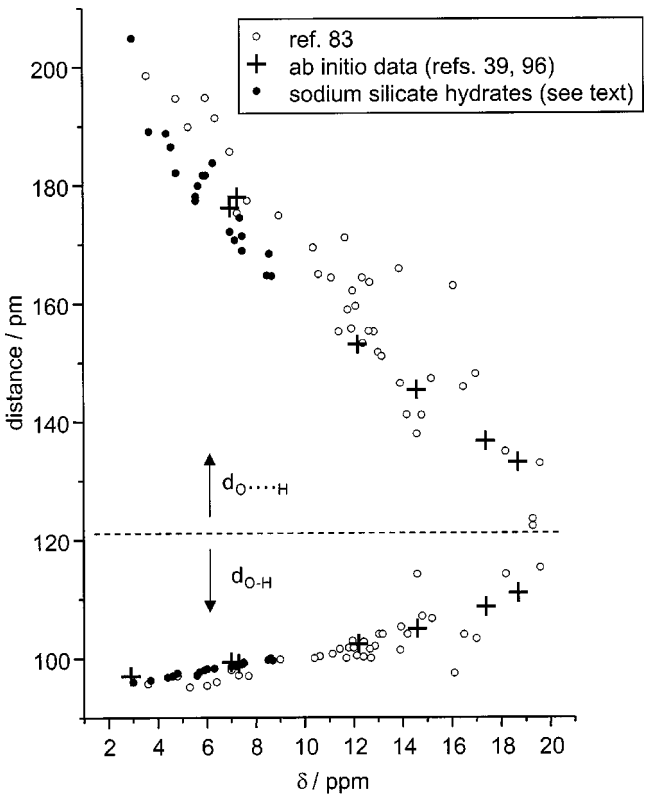

Figure 3. Correlation between the proton chemical shift in O–H···H hydrogen bonds and the covalent distance O–H (lower branch) or the hydrogen bond distance O···H (upper branch); data of Sternberg and Brunner and Sauer and coworkers are from [83] and [39,96], respectively.

The figure clearly shows that the predicted correlation between δ_H and d_{O-H} exists indeed.

3.1.2. Hydrogen bonds and proton chemical shifts of H_2O in sodium silicate hydrates

The O–H···O hydrogen-bond geometries with water molecules show a substantial structural variety [87–89]. Reports on experimental proton chemical shifts in structurally different water molecules in solid hydrates have hitherto been limited to averaged values due to the fast motion at room temperature. In order to study the sensitivity of ^{1}H chemical shifts for water molecules in hydrogen bonds in more detail, we have carried out ^{1}H MAS NMR experiments of the two sodium silicate hydrates $Na_2SiO_2(OH)_2\cdot 8H_2O$ and $Na_2SiO_2(OH)_2\cdot 4H_2O$ [90], which are known to contain nine and ten different hydrogen positions in the crystal structures with different O–H···O interactions [91,92], respectively. These sodium silicate hydrates have been very well characterized [93], and the absence of impurities in the highly crystalline samples was confirmed by ^{29}Si and ^{23}Na MAS NMR spectroscopy. At room temperature the different hydrogen sites cannot be distinguished in the ^{1}H MAS NMR spectra due the dynamic exchange of the protons of the water molecules. In order to avoid strong line broadening by homonuclear dipole interactions between the protons upon freezing the motion at low temperatures, the proton spin system has been diluted by deuteration (see, e.g., [94,95]).

The two sodium silicate hydrates were enriched in ^{2}H to about 95%, and the ^{1}H MAS NMR spectra were measured at 160 K (figure 4). Figure 4(a) displays the ^{1}H MAS NMR spectra for deuterated $Na_2SiO_2(OH)_2\cdot 8H_2O$. Nine sharp signals are identified which are superimposed on a broad background in the range between ca. 10 and 0 ppm. The origin of the broad line is not quite clear, but it may be due to residual ^{1}H–^{1}H pairs or by ^{1}H–^{2}H coupling. The nine sharp signals, shown in figure 4(b) after background subtraction, are assigned to the nine hydrogen positions in the structure. The baseline corrected ^{1}H MAS NMR spectrum of $Na_2SiO_2(OH)_2\cdot 4H_2O$, shown in figure 4(c), consists of six resolved lines with the relative intensities of 2 : 3 : 1 : 1 : 2 : 1 corresponding to the ten crystallographic sites. These results show that the dynamic averaging of proton chemical shifts of water molecules is frozen in the two sodium silicate hydrates by cooling the crystals, and all expected resonance lines appear in low-temperature ^{1}H MAS NMR experiments. In addition, the spectra displayed in figure 4 show that water molecules involved in different hydrogen-bonding produce ^{1}H NMR chemical shifts in a remarkably large range between ca. 3 and 9 ppm within these two structures; single-crystal neutron diffraction confirms that hydroxonium ions do not exist in these crystals [91,92]. The correlation between the proton chemical shift and the distances in the O–H···O hydrogen bonds (figure 3) is used in order to achieve an assignment of the signals in figure 4. The results are added to figure 3 as solid circles. These observations essentially show that H_2O has no unique

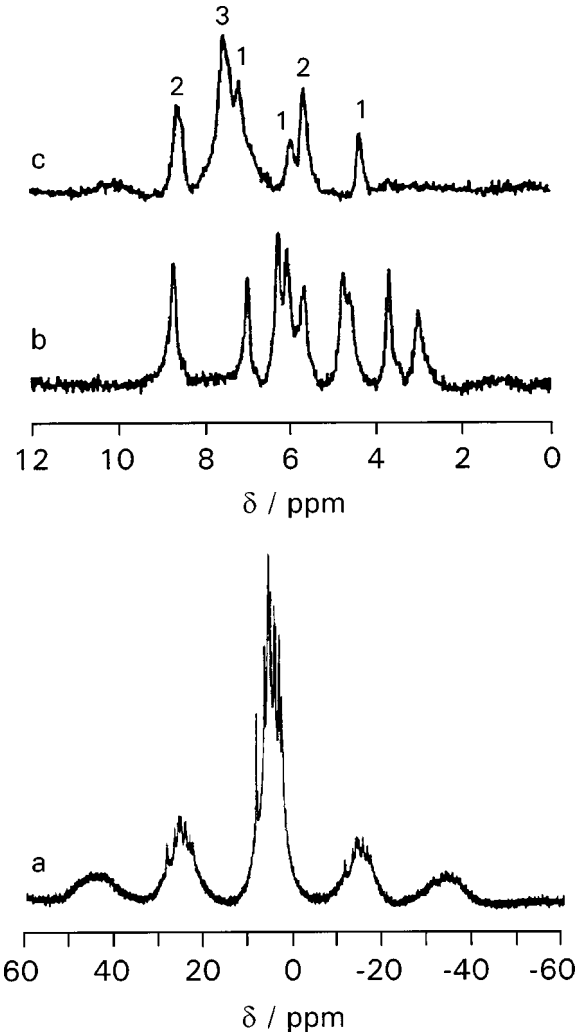

Figure 4. ^{1}H MAS NMR spectra (at 160 K) of the sodium silicate hydrates $Na_2H_2SiO_4{\cdot}xH_2O$; (a) $x = 8$, (b) $x = 8$ with baseline correction, (c) $x = 4$ with baseline correction (see text).

proton chemical shift in solids with hydrogen bonds. This can of course be envisaged from the work of Berglund and Vaughan [76]. Figures 3 and 4 nicely illustrate that even within a single well-defined structure a chemical shift range can appear which exceeds 6 ppm.

3.1.3. Hydrogen bonds and proton chemical shifts of water and methanol in zeolites from quantum-chemical model calculations

Next are discussed the ^{1}H chemical shifts of H_2O and methanol interacting with acidic zeolites in model clusters. Sauer and coworkers have calculated proton chemical shifts by Hartree–Fock based *ab initio* techniques in clusters which are models for a zeolitic Brønsted acid site interacting with H_2O or CH_3OH [39,96]. It was confirmed by the theoretical calculations that the ^{1}H chemical shift in this model system is sensitive to the hydrogen-bond geometry. The authors found that the calculated chemical shifts were only in good agreement with experimental results if they included electron correlation self-consistently. The two different scenarios sketched in scheme 2 were computed: the neutral adsorption complex (NC) and the ion pair structure (IP).

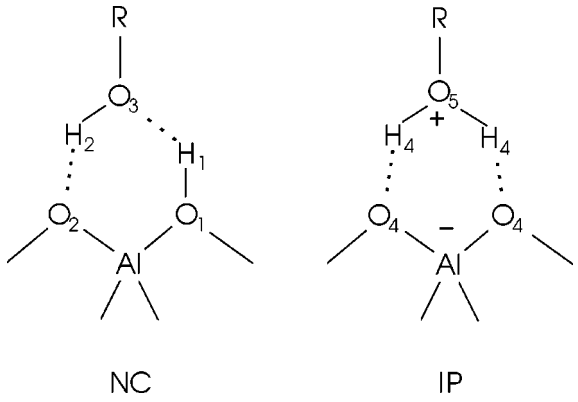

Scheme 2.

The zeolite was mimicked in these quantum-chemical calculations by a central $AlO^-_{4/2}$ tetrahedron which is surrounded by four SiH_3 groups, and a Brønsted proton. Selected interatomic distances of the four structures (R = CH_3 or H) of scheme 1 are listed in table 1 along with the calculated chemical shifts of the protons H1, H2 and H4. These ab initio data are also included in the correlation of figure 3 as crosses. The agreement between the quantum-chemical results with the experimental correlation in figure 3 is very good. This good fit makes the theoretical results to important reference data for an improved understanding of the experimental proton NMR work on H_2O or CH_3OH in zeolites on a molecular level. Note that even the data for the O–H bond of the free zeolite (table 1), which is not involved in any hydrogen bond, fit in the correlation of figure 3. Thus, the change in the chemical shift in the hydrogen-bonded structures is due to a structural change in the covalent O–H bond as a result of its interaction with a hydrogen-bond acceptor. This concept is ubiquitous also in the sense that the chemical shift is solely a function of local structure and not of the individual nature of the participating molecules; that means that the proton chemical shift in hydrogen bonds cannot be used as a parameter to discriminate a priori between the two structures, NC and IP, by proton NMR. A difference in chemical shift between the protons in the two structures, NC and IP (scheme 2), is due to the different strengths in hydrogen bonds. The particular hydrogen-bond structures must be well-defined to discriminate between the two scenarios by proton NMR. This condition is achieved by the quantum-chemical calculations in [39,96].

Most of the experimental proton NMR chemical shifts are dynamically averaged values, hence the quantum-chemically calculated chemical shifts of all interchangeable protons were averaged to compare theory and experiment [39,96]. For the neutral 1 : 1 water complex (scheme 2: R = H, NC), a proton NMR signal at 7.1 ppm (H1: 12.2 ppm, H2: 7.3 ppm, R = H: 1.8 ppm), and for the ion pair structure a value of 13.4 ppm (H4: 18.7 ppm,

Table 1
Selected O–H distances and calculated proton chemical shifts in zeolite clusters interacting with a water or methanol molecule; data are taken from [39,96] (shell-2.0, ab initio calculations including self-consistent electron correlation on MP2 level).

	Neutral adsorption complex				Ion pair complex	
	O1–H1	O3–H1	O2–H2	O3–H2	O4–H4	O5–H4
H_2O						
distance (pm)	102.4	153.0	178.0	99.1	133.0	110.9
δ_H (ppm)	12.2		7.3		18.7	
CH_3OH						
distance (pm)	104.9	145.3	176.2	99.3	136.6	108.6
δ_H (ppm)	14.6		7.0		17.4	
Bare zeolite						
distance (pm)	97.0					
δ_H (ppm)	2.9					

R = H: 2.7 ppm) have been calculated [39]. The results for the loading of one methanol molecule per acid site (1 : 1 complex) are 10.8 (H1: 14.6 ppm, H2: 7.0 ppm) and 17.4 ppm (H4 only) for NC or IP, respectively [96].

The ab initio calculations of Sauer and coworkers have shown, for a loading of one molecule (H_2O or CH_3OH) per acid site, that the neutral complex is a minimum structure and the ion pair complex is a transition state on the potential energy surface [39,96]. This result is in agreement with other theoretical reports using the cluster approach (see, e.g., [97–99]). Adsorption of a second water molecule per site (for R = H) changes this situation. Then, based on calculations using density functional theory, both structures are local minima, and a dynamic equilibrium between both is possible [39]. The use of the DFT method for the higher loading was validated by the good agreement between MP2 results on smaller complexes and density functional theory, using gradient corrected functionals. The anticipated averaged proton chemical shifts for the 2 : 1 complex with H_2O are 7.4 and 10.6 ppm for the neutral complex and the ion pair structure, respectively. Taking into account the possibility of an equilibrium between the neutral and the ion pair complex, Krossner and Sauer predict a change in the proton chemical shift from 7 to 9.0–10.6 ppm upon increasing the loading from one to two molecules H_2O per acid site. The result of these cluster calculations will be used now for the discussion of experimental data.

3.2. ^1H NMR spectroscopy of zeolites with adsorbed H_2O or CH_3OH

3.2.1. H_2O

For a comparison and for an easy reference, the ^1H chemical shift data discussed here are listed in table 2. ^1H MAS NMR experiments have been published by Luz and Vega [100] using zeolite H-Rho loaded with H_2O. The bare zeolite shows a ^1H MAS NMR signal at 3.6 ppm for the Brønsted sites. This line gradually disappeared upon approaching a loading of one H_2O molecule per Brønsted site, and new signals were observed, which vary in chemical shifts depending on the loading. At a loading of about one molecule per acid site, a broad peak at 7 ppm was observed besides a sharper line at 6.1 ppm. These lines are close to the value calculated in [39] for the neutral complex. It is not clear, however, why two signals were observed by Luz and Vega. At a loading of two H_2O molecules per Brønsted proton, two ^1H NMR signals with chemical shifts of 9.1 and 4.8 ppm were found. Only the latter line moves a little to 4.6 ppm, and its relative intensity grows upon further increasing the loading, but no further changes were observed at higher loaded samples. The line at 4.6 ppm was assigned by Luz and Vega [100] to liquid H_2O which does not strongly interact with the zeolite. The signal at 9.1 ppm agrees with the result of Krossner and Sauer [39] who predicted that partial proton transfer takes place at this loading with the corresponding averaged chemical shift (9.0–10.6 ppm), assuming a weighted averaging between the shifts of NC and IP (scheme 2).

Table 2
^1H chemical shifts of hydroxyl protons in acidic zeolites loaded with H_2O or CH_3OH.

Zeolite	Loading	Chemical shifts (ppm)	Reference
H_2O			
H-Rho	1 : 1	7.0, 6.1	[100]
H-Rho	2 : 1 to full	9.1, 4.8, 4.6	[100]
H-ZSM-5	1 : 1	5.8–6.2	[101]
H-ZSM-5	full	9.2, 5.0	[101]
CH_3OH			
H-Rho	<1 : 1	12	[100]
H-Rho	1 : 1	10.5	[100]
H-Rho	full	8.0, 4.3	[100]
H-ZSM-5	6 : 1	9.1, 4.1	[105]
H-ZSM-5	1 : 1	9.5 (at 153 K: 14.2, 4.1)	[106,107]
H-ZSM-5	3 : 1	8.5	[107]
HY	1 : 1	7.2	[106]

Hunger et al. [101] have investigated by ^1H MAS NMR spectroscopy the sorption of H_2O in zeolite HY. For loadings close to one molecule per acid site these authors observed a proton chemical shift of 5.8–6.2 ppm. At full loading the main signal was at 5.0 ppm besides a smaller component at 9.2 ppm. These observations resemble those of Luz and Vega. However, Hunger et al. have suggested

to assign the line at 9.2 ppm to protons in $Al(H_2O)_6^{3+}$ extra-framework complexes [101]. A signal at 6.5 ppm in hydrothermally dealuminated zeolite HY was assigned to water molecules at Lewis acid sites. Deng et al. have recently adapted this assignment in a $^1H/^{27}Al$ TRAPDOR NMR study [102].

Comparison of the experimental ^1H NMR chemical shifts in zeolites loaded with one H_2O molecule per acid site (5.8–7.0 ppm) [100,101] with the theoretical calculations [39] (7.1 ppm for NC and 13.4 ppm for IP) clearly suggests that the neutral complex (NC) structure of scheme 2 is favored for the 1 : 1 complex over the ion pair structure. A clear conclusion for higher loadings cannot be made at this point due to the mentioned ambiguities with extra-framework aluminum in experimental studies.

Another approach has been suggested by Batamack et al. [103] using zeolite HY. These authors utilized homonuclear dipole interactions between protons, instead of analyzing their chemical shifts. H_2O with its two protons is a two-spin system, whereas H_3O^+ represents a symmetric three-spin system which may be slightly distorted in the adsorbed state. Isolated acid protons as single spins and O–H$\cdots$$H_2O$ as an asymmetric three-spin model for the neutral adsorption complex at the Brønsted site were considered as well. For these model structures the expected dipole interaction between the protons can be calculated by analytical equations. This method allows for a prediction of experimental lineshapes in ^1H NMR spectra of stationary samples, when molecular motion is frozen at a temperature of 4 K. The analytic lineshape functions were fitted to the experimental spectra, resulting in a quantitative analysis of the number of H_2O, H_3O^+, O–H$\cdots$$H_2O$ and OH species per unit cell. The heteronuclear dipole interaction between ^1H and ^{27}Al is neglected in this model. In addition, multi-spin systems in water clusters are too complicated to be treated analytically. Two or more water molecules per acid site were, therefore, not considered in the analytical model of Batamack et al. This drawback could matter for loadings higher than one molecule per acid site, but it is not a problem for small loadings. For loadings up to a 1 : 1 coverage, the dominating species is found to be the neutral adsorption complex, besides unaffected Brønsted sites, which is in agreement with the aforementioned results from proton chemical shifts. However, H_3O^+ ions were also observed to about one fourth of the amount of neutral complex [103]. This is yet another evidence for the existence of both, the neutral and the ion pair complex, within a single structure. Recall that Smith et al. [38] have also found both cases in H-SAPO-34 by neutron diffraction.

The conclusion from ^1H NMR spectroscopy on the adsorption of H_2O in acidic zeolites is that the neutral adsorption complex is the dominant one at low loadings up to one molecule per acid site, but small amounts of the ion pair structure are possible. For higher loadings an unambiguous conclusion cannot be drawn based on ^1H NMR experiments.

3.2.2. CH_3OH

^1H MAS NMR spectra of methanol adsorbed in an acidic zeolite have been published by Luz and Vega [100]. The loadings of methanol (as deuterated CD_3OH) adsorbed in zeolite H-Rho were varied between low (ca. 0.5 molecules per acid site) and high loading (ca. 3.5 molecules per Brønsted proton). A proton NMR signal at 12 ppm was observed at the lowest loading (table 2) which is shifted to ca. 10.5 ppm and increases in intensity at a coverage of one molecule CH_3OH per acid site. Concomitantly with this observation, the line for the uncovered acid sites at 3.6 ppm gradually disappeared. At full loading with methanol, the signal at 10.5 ppm moved upfield to 8 ppm. For loadings of more than two molecules per acid site, another line at 4.3 ppm appeared which was assigned to free methanol. The shift of the main signal from 12 to 8 ppm has been explained by diminishing hydrogen-bonding of the intracavity methanol molecules.

Proton MAS NMR experiments of methanol in H-ZSM-5 have been published by Mirth et al. [104] and Anderson et al. [105]. Chemical shifts of 4.1 ppm for the methyl group and of 9.1 ppm (table 2) for the averaged signal for the OH groups of methanol and the Brønsted site have been reported for H-ZSM-5 with a high loading of six molecules per acid site [104]. At lower coverages, a downfield shift to 10.5 ppm occurred [104]. Interestingly, the chemical shift values of the methanol OH group in H-ZSM-5 at room temperature and in the liquid superacid FSO_3H–SbF_5–SO_2 at $-60\,^\circ C$ are the same [105]. However, it should be noted that the comparison between chemical shifts in zeolites and in the superacid does not prove the protonation of methanol in a zeolite. The proton chemical shift depends on the hydrogen-bond donor and acceptor properties, as has been explained in detail in section 3.1. Recall that, for instance, the water molecules in the sodium silicate hydrates produce a rather large chemical shift range (3–9 ppm) without any protonation, depending solely on the strength of the hydrogen bonds.

A set of proton chemical shift data were reported for the hydroxyl group of methanol in a series of zeolites [105] saturated with methanol. The shifts ranged between 3.8 ppm for the siliceous form of ZSM-5 without Brønsted protons (silicalite-1) and 9.4 ppm for the same zeolite but with acid sites (H-ZSM-5). This observation is a clear indication for the stronger hydrogen-bond interactions between methanol (or protonated methanol) and the different acceptor systems ZSM-5 and silicalite-1.

Hunger et al. found a chemical shift of 9.5 ppm for a coverage of one molecule per acid site in H-ZSM-5 [106,107]. This signal was assigned to neutral methanol molecules which are hydrogen-bonded to the acid site. At a loading of three molecules CD_3OH per acid site in H-ZSM-5, a signal at 8.5 ppm has been observed [107]. Similar experiments on a dealuminated zeolite H-Y (Si/Al = 8.0) resulted in a shift value of 7.2 ppm for a 1 : 1 loading [106]. It was found that the species associated with these lines must have a high mobility. Small amounts of stronger bound mole-

cules were detected by spectral editing techniques [107]. In addition, these authors have carried out ^{1}H MAS NMR experiments at low temperatures. At 153 K the line with a chemical shift of 9.5 ppm in H-ZSM-5 has disappeared and two other resonances at 14.2 and 4.1 ppm occurred instead. This result suggests that the dynamic exchange between the two corresponding sites has been frozen at this temperature, and the signal at 9.5 ppm at room temperature corresponds to the averaged value. The chemical shift values at 14.2 and 4.1 ppm are in reasonable agreement with the calculated ones for the neutral adsorption complex (without exchange) by Haase and Sauer (14.6 and 7.0 ppm), at least for proton H1 (table 1).

Hunger and Horvath have also studied the higher loading of three molecules per acid site at low temperatures [107]. A signal at 16.5 ppm has been observed at 153 K. This chemical shift could be due to methoxonium ions, since Haase and Sauer [96] have calculated a value of 17.4 ppm for this species. However, it should be borne in mind that the calculation has been carried out for the 1 : 1 complex, and the experimental value of 16.5 ppm has been obtained for a 3 : 1 loading. We are not aware of calculated chemical shifts for a 3 : 1 loading with methanol.

All cited authors have observed proton chemical shifts ranging between 7.2 and 10.5 ppm for a 1 : 1 loading of methanol in several zeolites. In conjunction with the theoretical calculations, these results allow for the conclusion that the dominant species at low loadings (1 : 1 complex or lower) is the neutral adsorption complex (NC). It is interesting that the proton chemical shifts suggest stronger hydrogen bonds of methanol in HZSM-5 compared to HY. Using the concept outlined above, the ZSM-5 framework must be a stronger hydrogen-bond acceptor or donor than zeolite Y.

For higher loadings no clear conclusion can be drawn. There is a lack of high-quality model calculations (e.g., ab initio calculations on the MP2 level of theory) for loadings higher than 2 : 1. Interaction between different methanol molecules can influence the adsorption behavior [108], and chemical exchange can occur. In addition, there is another ambiguity by the yet unanswered question whether a methoxonium ion could be formed at higher loadings, donating two hydrogen bonds to two methanol molecules. A dynamic exchange between different interacting species could also occur. Questions like these make the whole scenario more complicated. However, there is a clear fundamental difference when H_2O or CH_3OH is adsorbed in acidic zeolites: upon increasing the loading, the average proton chemical shifts in the methanol case shift to high field, and H_2O shows the opposite trend (table 2). This observation means that the average hydrogen-bond strength of the hydroxyl groups increases for water and decreases for methanol with higher loadings. This is a possible hint at differences between the two probe molecules in their proton affinity as the protonated molecules form obviously stronger hydrogen bonds [39,96] with the zeolite.

Another evidence for the importance of loading levels of methanol is provided by the static low-temperature ^{1}H NMR method of the Fraissard group. If the coverages is lower than one molecule per acid site, then only the neutral complex has been observed [109].

3.3. ^{2}H NMR spectroscopy

Due to its nuclear electric quadrupole moment, the deuterium nuclei have NMR properties that differ from those of protons. ^{2}H NMR spectra are often measured on stationary samples (no magic angle spinning), because the obtained quadrupolar lineshapes are of particular interest. The linewidth in rigid solids is a function of the strength of the nuclear quadrupole interaction which depends on the local electric field gradient at the deuterium [110–112]. This anisotropic nuclear spin interaction provides a wealth of information of dynamic processes. Isotropic motions can be distinguished from anisotropic motions, and even mechanisms of anisotropic processes and their time scale can be studied.

If the deuterons are involved in O–D$\cdots$O hydrogen bonds, then the local electric field gradient at the deuteron is a function of the strength of the hydrogen bond [76] which makes the quadrupole interaction (the linewidth) very informative about this bond. Berglund and Vaughan found a linear correlation between the proton chemical shift and the square of the quadrupole coupling constant in O–H(D)$\cdots$O hydrogen bonds. The shorter the O$\cdots$O distance in the hydrogen bond the smaller is the deuterium quadrupole coupling constant, corresponding to proton (or deuterium) chemical shifts being downfield.

Luz and Vega used ^{2}H NMR spectroscopy for protonic zeolites with defined amounts of adsorbed D_2O [100]. However, these experiments were not very informative as to the structure of the adsorption complex, because a dispersion of several sites with varying degrees of motional freedom and strengths of hydrogen-bonding of D_2O contribute to complex ^{2}H NMR lineshapes. Therefore, the subsequent considerations are confined to methanol.

Deuterated hydroxyl groups, in particular the zeolitic acid site and the methanolic OD group, undergoing fast dynamic exchange with each other, have been investigated by Hunger and Horvath [107,113]. In order to reduce motional narrowing, the experiments were carried out at 85 K for 1 : 1 and 3 : 1 loadings of ZSM-5. At a 1 : 1 loading two quadrupole powder patterns have been observed (figure 5). A broad quadrupolar pattern is characterized by a deuterium quadrupole coupling constant of 230 kHz. Another component has been observed with a quadrupole coupling constant of 140 kHz for hydroxyl groups in strong hydrogen bonds (figure 5). This component corresponds to the proton NMR line of the same sample at 14.2 ppm according to the correlation in [76], while the broad pattern is consistent with the proton chemical shift at 4.1 ppm. This latter component in the ^{1}H MAS NMR spectrum at 153 K and in the deuterium NMR spectrum at 85 K may suggest the

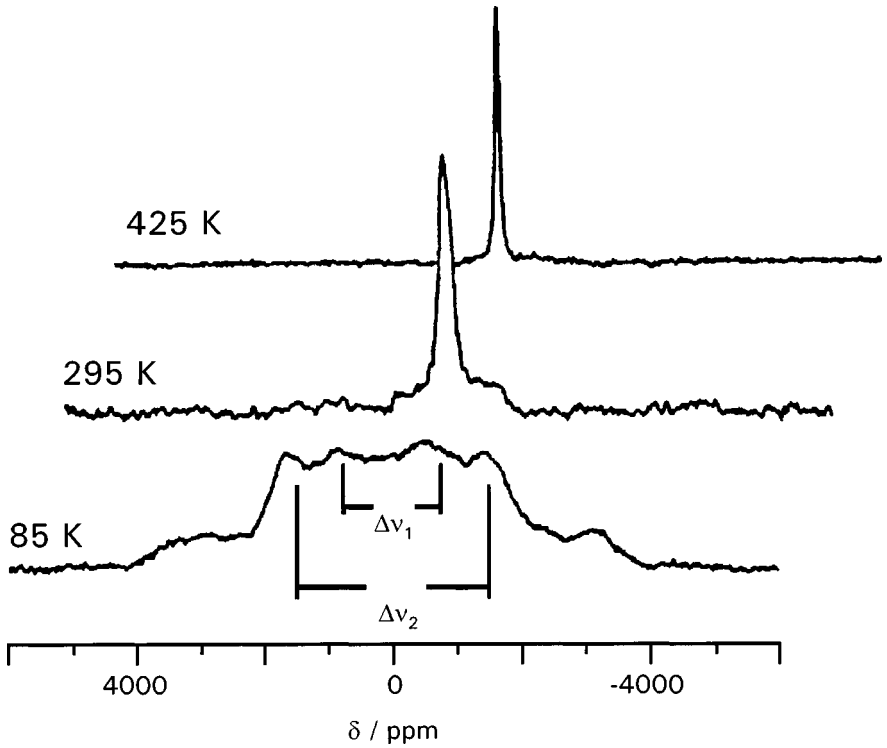

Figure 5. ^{2}H NMR spectra of CH_3OD adsorbed at the acid site of H-ZSM-5 (1 : 1 loading), reprinted with permission from [107], copyright 1996 American Chemical Society.

presence of unaffected or only weakly affected acid sites, although the average loading was 1 : 1. This observation raises the question whether clustering of methanol molecules has occurred, and, at least for low temperatures, not all of the acid sites were covered. Alternatively, the broad deuterium NMR signal is due to the deuterated hydrogen atom H_2 in scheme 2, as the ^{1}H NMR line at 4.1 ppm has been assigned to this proton [107]. At higher temperatures all broad ^{2}H NMR components are narrowed by dynamic motion, and merge to one sharp line at a temperature of 425 K (figure 5). This observation shows that all hydroxyl groups now take part in dynamic exchange. At room temperature the ^{2}H NMR spectrum consists of a sharp line in addition to a broader component (figure 5). The latter could correspond to the proton NMR line of rigid sites which has been detected by spectral edition experiments associated with the main components in the ^{1}H MAS NMR spectra at room temperature [106,114].

Additional information as to the dynamics of methanol is provided by ^{2}H NMR spectra with deuterated methyl groups [100,113]. Luz and Vega concluded from ^{2}H NMR experiments of CD_3OH in zeolite H-Rho (loading 1 : 1 or lower) that the methyl group probably undergoes some librational motion about an axis which is perpendicular to the C–O bond [100]. The extent to which this libration occurs depends on the loading and on the temperature which has been varied between 173 and 423 K. The librational angle seems to be distributed. A possible mechanism for such a librational motion is speculated in figure 6 which keeps the entire molecule adsorbed, but allows for a local motion which could explain the observations by Luz and Vega. Interestingly, this librational motion is not observed by the ^{2}H NMR experiments with ZSM-5 at a temperature as low as 85 K [113]. The quadrupole coupling constant of 37 kHz of a well-defined lineshape clearly indicates that the methyl group rotates only about its internal threefold axis. Similar observations have been reported by Šepa et al. [115]. These authors have looked at the methyl group rotation of acetonitrile adsorbed in H-ZSM-5 (1 : 1 loading) by analyzing dipolar lineshapes in static proton NMR spectra, and they found at 78 K a rotation about the internal C_3 symmetry axis of the methyl group. At higher temperatures a reorientation of this rotation axis was observed as an additional motion, and a motion similar to the one shown in figure 6 was assumed [115,116]. The intrinsic potential energy surface for the motion sketched in figure 6 is not known to the best of our knowledge. At least for a small librational motion about the equilibrium orientation the potential is assumed to be quite shallow, and such a motion should be easily possible, if no other interactions were present. However, such a process could be hindered by the interaction of the methyl group with the "zeolite wall". Interestingly, different zeolitic effects on the activation of the isotropic reorientation of acetonitrile have been observed by White and coworkers [116]. The observed differences for different zeolites can be due to steric confinement, or due to the aforementioned interaction between the methyl group and the zeolite framework. For a theoretical study of the Van der Waals interaction between the methyl group and the zeolite wall, the cluster size would

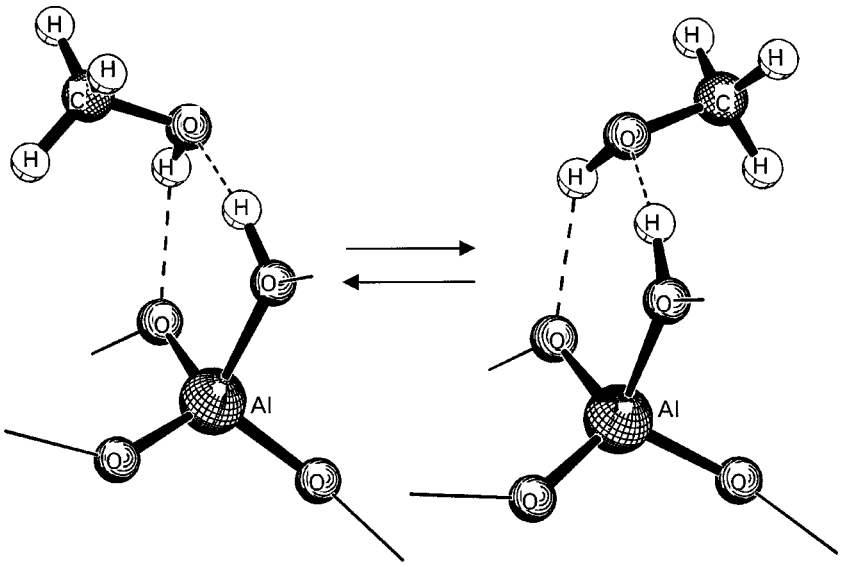

Figure 6. Model of methyl group motion of methanol adsorbed on the acid site.

have to be increased. An influence of the methyl group interaction within the zeolite is also anticipated by Haase and Sauer [96], who calculated an increasing adsorption energy for an increasing cluster size. Clearly, more work has to be done in order to study molecular motions of methanol in zeolites as shown in figure 6. Recently, a similar quadrupolar line of methyl groups undergoing only a rotation about its internal axis has been found by Salehirad and Anderson in H-SAPO-34 at room temperature [52]. In this case the line has been assigned to surface methoxy groups which have been formed at 473 K. The chemical bond of the methyl group to the surface prevents librational mobility.

In summary, the proton and deuterium NMR work consistently probes the hydrogen-bonding of the surface adsorption complex of CH_3OH in zeolites. For a 1 : 1 loading the hydrogen-bonded neutral complex dominates over the ion pair structure. Probably, several motional degrees of freedom have to be considered for an even more detailed analysis. In the next section we will attempt to introduce a few dynamic models with the intent to help stimulate further studies. It is difficult to unequivocally prove the presence of several motional mechanisms solely based on a single experiment. The comparison between different experiments with a collection or interplay of evidences is imperative. In addition, molecular dynamics studies can help to discriminate between different motional models in the future.

3.4. ^{27}Al NMR spectroscopy

It has been thought for a long time that the study of zeolitic acid sites would be hardly feasible by ^{27}Al NMR spectroscopy of dehydrated samples. The resonance line of these sites was broadened beyond the detection limit in conventional ^{27}Al MAS NMR spectra and the term "invisible aluminum" has been used. The reason for this line broadening is based on the nuclear electric quadrupole moment of ^{27}Al which interacts with a local electric field gradient (quadrupole interaction).

By applying a NMR echo technique Ernst et al. [117] were able to measure for the first time the broad ^{27}Al NMR line of zeolitic acid site in dehydrated stationary samples (no magic angle spinning). The corresponding quadrupole coupling constant in H-ZSM-5 was 16 MHz. Other groups found values in protonic zeolites ranging between 11 and 18 MHz [102,106,107,113,118,119]. These values are unusually large for a tetrahedral aluminum coordination [118]. Since the quadrupole coupling constant is a direct measure for the local electric field gradient, it provides local structural information. The line broadening is due to structural strain, introduced by protonation, which is reduced upon adsorption of water or methanol at the Brønsted site, and thus ^{27}Al MAS NMR spectra can be measured of loaded zeolites [100,101,120–122]. Upon adsorption of one methanol per acid site the overall ^{27}Al NMR linewidth of a stationary sample decreases, and a quadrupole coupling constant of 8.0 ± 0.5 MHz is observed, i.e., a reduction by about a factor of 0.5 occurs compared to the unloaded protonated zeolite. Similarly reduced values were found in zeolites loaded with ammonia or pyridine, which are known to deprotonate the zeolite framework [106]. It is tempting to conclude that the similar reduction of the ^{27}Al quadrupole coupling constant upon adsorption of NH_3, pyridine or methanol indicates the formation of methoxonium ions. However, this conclusion is apparently not consistent with the aforementioned results from ^{1}H NMR spectroscopy. It will be shown that dynamic effects must not be neglected, as they can reduce the quadrupole interaction of ^{27}Al by a motional process. The recognition that a dynamic process at the acid site can reduce the quadrupole coupling constant of ^{27}Al has not been sufficiently considered in the literature so far, and this could lead to misinterpretations of experimental data. In what follows, the underlying principles of the structural strain and its relaxation upon adsorption of

molecules will be discussed. The results of these considerations add to the left side of figure 1, as they address the local structure of aluminum in scheme 1 with and without adsorbed probe molecules.

The line broadening and the large quadrupole coupling constant in ^{27}Al NMR spectra of dehydrated H-zeolites are due to a large electric field gradient (efg) at the aluminum nucleus. This efg originates from the distorted bonding environment of the aluminum [123]. For tetrahedral symmetry the electric field gradient would be spherically symmetric and a quadrupole interaction would not occur. In order to understand the large quadrupole coupling constants of ^{27}Al for the zeolitic acid sites, and the observed changes upon adsorption of probe molecules [106], quantum-chemical calculations have been carried out on model clusters using density functional theory [123]. The free zeolite cluster is displayed in figure 7. It was found that the coordination of aluminum is not tetrahedral in the protonated zeolite, as has been shown before by several other groups [7,10,13,96,97]. Instead, a bonding situation as sketched in scheme 1 is observed, where Al has a coordination number between three and four, based on bond order criteria. These bond properties change when a probe molecule interacts with the acid site. The probe molecule interacting with the Brønsted proton weakens the O–H bond, and, according to the bond order conservation principle, the O–Al bond order increases in order to maintain the oxygen valence [13]. As shown in [123] the variation of the Al–O bond orders correlates well with relative changes of the quadrupole coupling constant of ^{27}Al, for instance, when probe molecules are adsorbed on the acid site. Thus, the relative strength of the quadrupole interaction of ^{27}Al is a measure of the relative strength of the interaction of a molecule with the acid proton, if dynamic effects do not play a role. The adsorption of a neutral methanol molecule cannot account for the reduction of the quadrupole coupling constant of ^{27}Al by a factor of about 0.5 [123]. On the contrary, an ion pair complex would explain the observed changes for a 1 : 1 loading with methanol, but dynamic effects have to be considered before any conclusion can be made on the protonation of methanol.

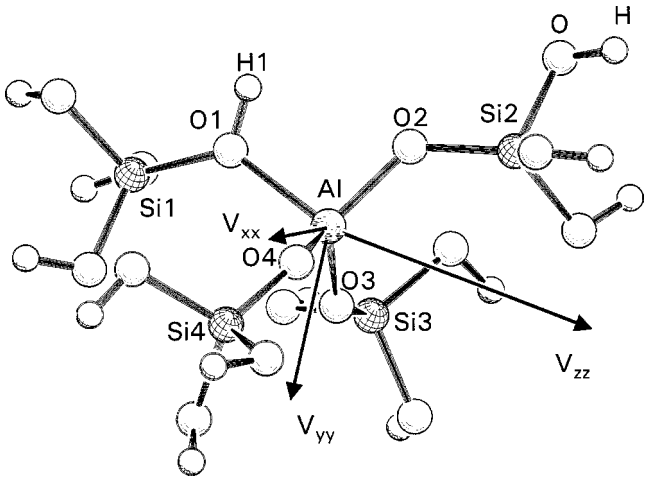

Figure 7. Zeolite cluster used for calculations of electric field gradients at aluminum.

The electric field gradient tensor is reduced by dynamic motion, depending on mechanism and time scale of the dynamic process. To account for this we need to know the time-dependent orientation of the efg tensor in the dynamic exchange. This is not an easy task, since the mechanisms of molecular motion of methanol in zeolites are unknown. As has been pointed out in section 3.3, more work has to be done in order to understand the molecular motion of CH_3OH in zeolites. Nevertheless, we present here some alternative motional models which could rationalize the observed line narrowing in the ^{27}Al NMR spectra.

The largest component of the electric field gradient tensor in the zeolite cluster, V_{zz}, is nearly in the same direction as the O1–Al interatomic vector (figure 7) [123]. This principal tensor orientation does not change much when a static methanol molecule interacts with the acid site. Figure 8 illustrates two symmetry equivalent local structures of a neutral methanol molecule adsorbed on a Brønsted acid site. The potential barrier for a dynamic exchange between the two structures has been calculated by ab initio and density functional techniques [96,97]. The activation energy for a two-site jump, as displayed in figure 8, is on the order of 10 kJ/mol. This low value means that such a process is very reasonable to occur, and its influence on the quadrupole interaction and the corresponding ^{27}Al NMR linewidth can be estimated. For such a two-site jump the efg principal tensor orientation jumps about the angle φ, and the averaged interaction tensor is for fast motion simply obtained by averaging the two different tensors in the different orientations. These calculations of averaged tensors for two-site jumps about different angles, φ, have been carried out by several authors. A graphical solution can for instance be found in the book of Schmidt-Rohr and Spiess [112]. Figure 9 shows the averaging effects, depending on the angle φ, of a fast two-site jump resulting in the motionally averaged asymmetry parameter, $\langle\eta\rangle$, and the reduction of the quadrupole coupling constant, QCC, by the factor of $|\langle\mathrm{QCC}\rangle|/\mathrm{QCC}$ [112]. The quadrupole coupling constant is reduced by a factor of 0.5 (figure 9), when the angle φ is between 70.6 and 109.5°. The jump angle φ is defined by the O–Al–O angle which is around 95–100° in figure 8 according to the calculations by several authors (see, e.g., [96,97,123]). These considerations show that a two-site jump of the Brønsted proton (figure 8) can explain the observed reduction by a factor of about 0.5 of the quadrupole coupling constant of ^{27}Al, when a neutral methanol molecule is adsorbed at the acid site. However, based on the calculations in [123] the same value would be expected for the ion pair structure with rigid methoxonium ions. Therefore, ^{27}Al NMR spectroscopy cannot distinguish a priori between the two cases NC or IP (scheme 2). Due to the additional evidence from ^{1}H and ^{2}H NMR it must follow that a single methanol molecule is adsorbed as a neutral species which takes part in an exchange process of the Brønsted proton. The role of methanol in this proton

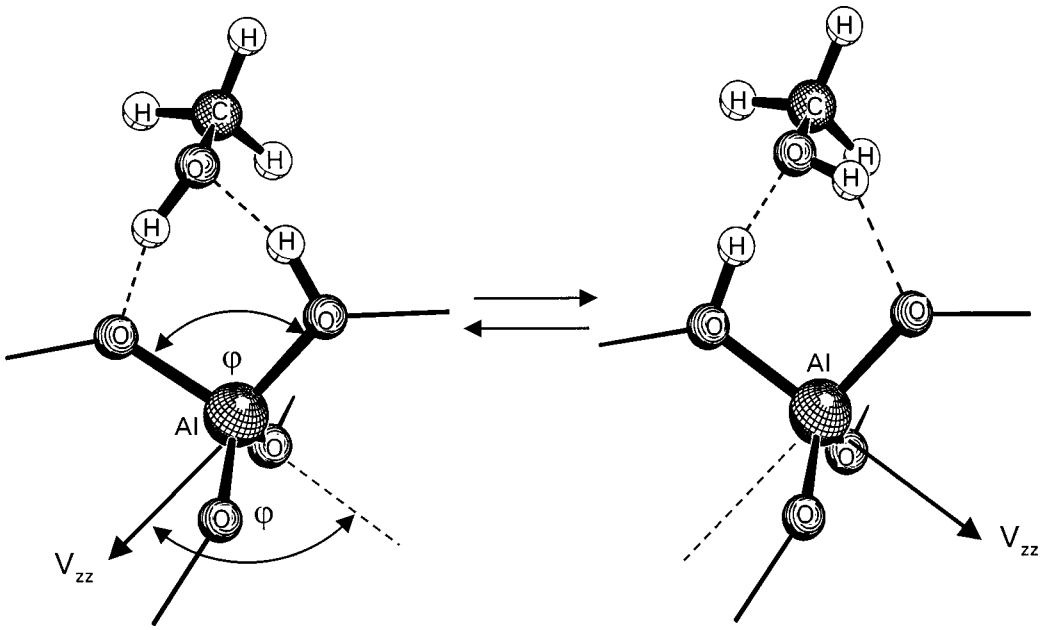

Figure 8. Model of dynamic exchange between the two hydroxyl groups inducing a motion of the electric field gradient tensor at aluminum.

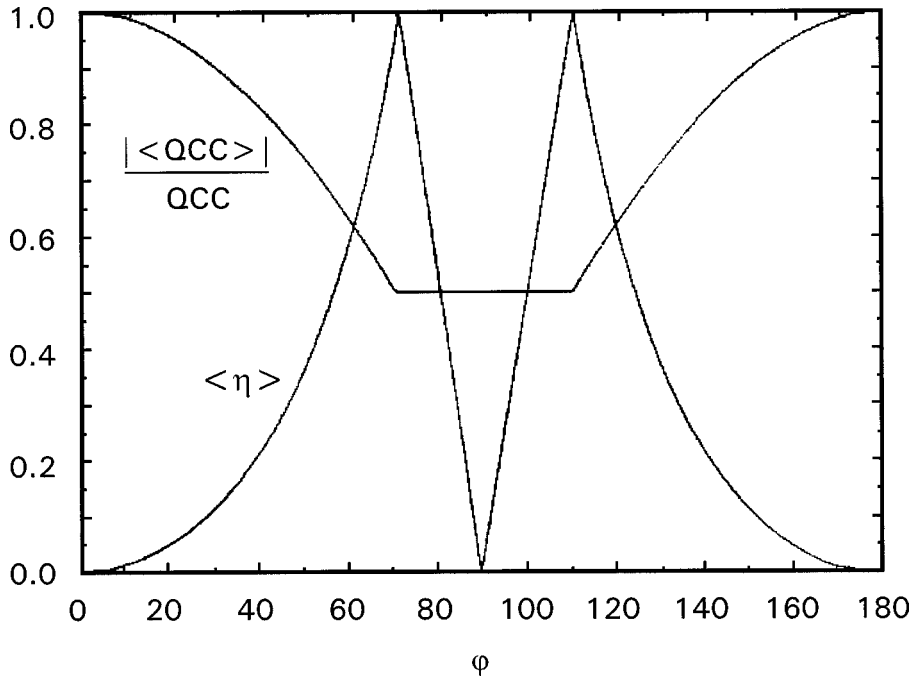

Figure 9. Reduction factor of the quadrupole coupling constant and asymmetry parameter of the electric field gradient for a two-site jump process about an angle φ; reprinted from [112], by permission of the publisher Academic Press Limited, London.

jumps needs to be clarified, but as one first possibility the mechanism shown in figure 8 is considered.

However, this two-site jump model displayed in figure 8 is not supported by the ^{1}H and ^{2}H NMR data at low temperatures presented in the preceding sections. It has been shown that the two hydrogens do not undergo this exchange at low temperatures. The two protons would average between two hydrogen bond strengths, a strong and a weak hydrogen bond, which would result in a single ^{1}H and ^{2}H NMR line. The observation of two lines instead indicates that the process shown in figure 8 cannot explain the ^{1}H and ^{2}H NMR data at low temperatures, although it would help to understand the ^{27}Al NMR spectra.

Therefore, an alternative model is presented in figure 10. The basic idea is that the weak hydrogen bond between the methanol OH group and the zeolite framework is one position further away from the aluminum. Such an adsorption complex has been suggested by Haase et al. and Nusterer et al. [44,123]. If the Brønsted proton exchanges between the two oxygen positions O1 and O2, then the electric field

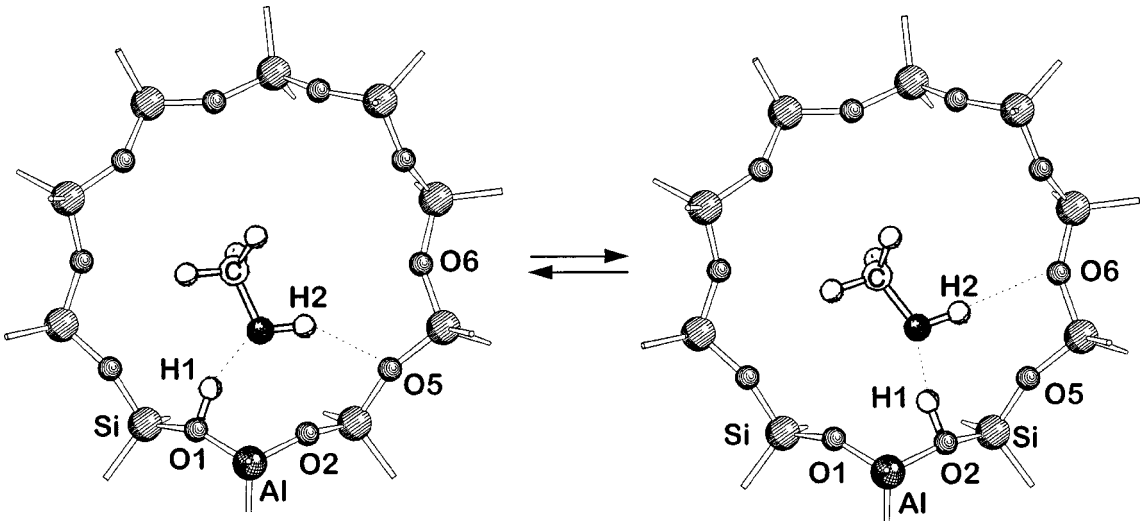

Figure 10. Motional model of methanol adsorbed at the acid site within a ten-membered ring of H-ZSM-5.

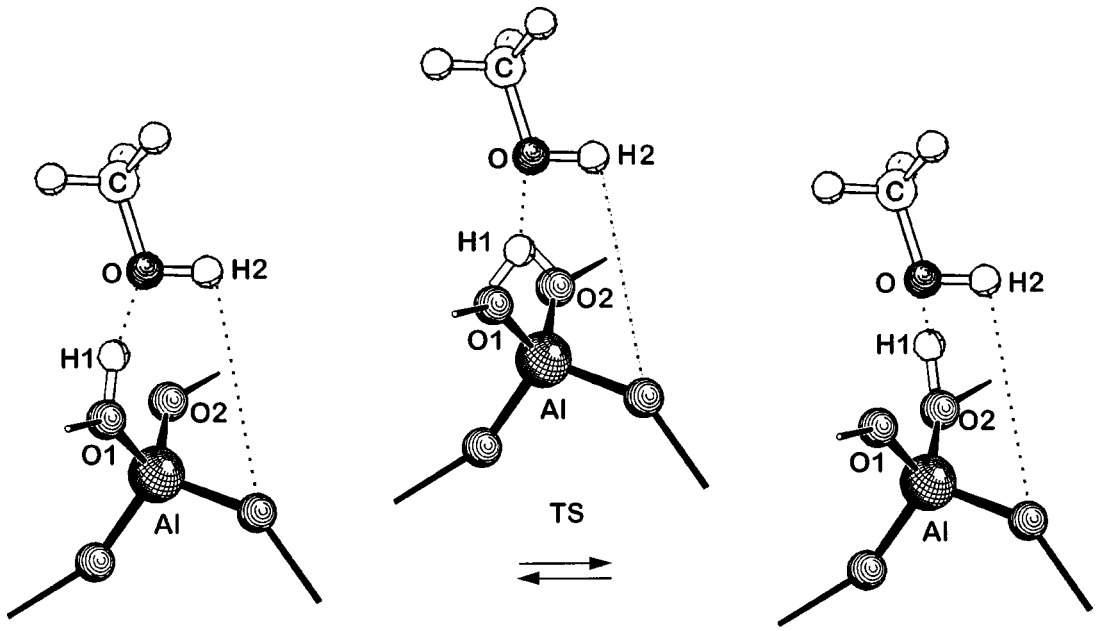

Figure 11. Motional model of methanol with three zeolitic oxygen atoms included.

gradient for aluminum would average in the same way as discussed for the process in figure 8. However, the NMR properties of the two hydrogen sites would not be averaged, since H1 would remain in a strong hydrogen bond for both configurations and H2 would be weakly hydrogen bonded for both structures. They would be distinguishable by ^{1}H and ^{2}H NMR.

This alternative model, which includes a concerted riding motion of the Brønsted proton and the methanol molecule, is now consistent with $^{1}H/^{2}H$ as well as ^{27}Al NMR data of the acid site interacting with one methanol molecule. Clearly, more evidence is needed to prove such a model, but it could help to stimulate and design further experiments.

There is yet another possible motion that is consistent with the described NMR data which we call a promoted single-proton jump (figure 11). In this process, three oxygen atoms of a $AlO_{4/2}^{-}$ center participate in the motion of the adsorption complex. In this process, the methanol molecule remains more or less at the same position with its oxygen atom centered above O1 and O2. The strong hydrogen bond interaction between the methanol oxygen and H1 promotes a fast motion of the proton between O1 and O2 without the need of much methanol motion. In the transition state (TS), the proton H1 is between the methanol oxygen atom and the center of O1 and O2. Again, the two protons, H1 and H2, differ in their ^{1}H NMR characteristics, and the efg at the aluminum nucleus would be averaged by the two-site jump of H1, in agreement with experimental data. The scenario is further complicated if the potential energy diagram of the proton exchange process is asymmetric, such as shown in figure 2(b).

We are not able to decide here which is the correct type of motion, but it is hoped that the presented models will help to fertilize future experimental and theoretical work.

In any case, one conclusion is absolutely clear: the ^{27}Al NMR spectra of zeolites with adsorbed molecules cannot be reasonably interpreted without the consideration of dynamic motion.

4. Summary

The combined use of solid-state NMR techniques and quantum-chemical calculations has been presented as a synergistic set of tools. The adsorption of H_2O and CH_3OH in acidic zeolites has been selected as a case-in-point for demonstrating the strategies when dynamic phenomena are studied with these methods.

The characterization of proton transfer processes is not trivial, but major achievements have been made in the last few years. Proton NMR chemical shifts are very informative as to the strength of the interaction between the zeolite framework and the species in the channel system, but they are a priori unsuitable at distinguishing between protonated and unprotonated probe molecules. However, the proton chemical shift can be used to this end, if the strength of interaction between the zeolite and the protonated or unprotonated molecule is known from other sources, for instance from quantum-chemical ab initio calculations. The consideration of the loading level is absolutely necessary to understand the experimental data. The average hydrogen-bond strength increases when the loading with water molecules in acidic zeolites increases, while it decreases with increasing loading with methanol. This observation hints at differences in the proton affinities of the two molecules with higher loadings. In the range of low loadings (1:1 coverage or lower) the hydrogen-bonded neutral complexes are minima on the potential energy surface in theoretical calculations and the protonated molecules are transition states, when the local properties of the zeolite acid site dominate the adsorption complex. However, experimental results indicate that both, the protonated and unprotonated probe molecules, are possible even for low loadings. This observation can be rationalized by including larger spacial surroundings of the Brønsted proton. The theoretical understanding of such matrix effects requires the consideration of larger zeolite models in quantum-chemical calculations, which is a very demanding condition for the computer performance and the methods available to date. However, the developments in recent years open the possiblity for important breakthroughs in the application of computational chemistry to zeolite catalysts, and the questions raised here are a motivation to pursue and follow the work in future years.

Several dynamic models are introduced for the adsorption complex of methanol in zeolites. The different cases considered have implications on a deeper understanding of adsorption and catalysis in zeolites which necessitates further experimental and theoretical work. The dynamics of hydrogen bonds is an important parameter to understand proton transfer in zeolites.

Acknowledgement

This work was funded by the European Union (contract ERBCHBGCT930309), by the Fonds der Chemischen Industrie and the German Bundesministerium für Bildung, Wissenschaft, Forschung und Technologie.

References

[1] (a) P.B. Weisz and V.J. Frilett, J. Phys. Chem. 64 (1960) 382;
(b) N.Y. Chen, W.E. Garwood and F.G. Dwyer, *Shape Selective Catalysis in Industrial Applications* (Dekker, New York, 1989);
(c) P.R. Pujadó, J.A. Rabó, G.J. Antos and S.A. Gembicki, Catalysis Today 13 (1992) 113;
(d) J.M. Thomas, Angew. Chem. Int. Ed. Engl. 33 (1994) 913;
(e) M.E. Davis, Acc. Chem. Res. 26 (1993) 111.
[2] A. Corma, Chem. Rev. 95 (1995) 559.
[3] W.F. Hölderich, J. Röseler, G. Heitmann and A.T. Liebens, Catalysis Today 37 (1997) 353.
[4] J.F. Haw, J.B. Nicholas, T. Xu, L.W. Beck and D.B. Ferguson, Acc. Chem. Res. 29 (1996) 259.
[5] (a) J.A. Rabó and G.J. Gajda, Catal. Rev. Sci. Eng. 31 (1990) 385;
(b) G.J. Gajda and J.A. Rabó, *ASI on Acidity and Basicity of Solids: Theory, Assessment and Utility*, Nice, 1993.
[6] W.J. Mortier, J. Sauer, J.A. Lercher and H. Noller, J. Phys. Chem. 88 (1984) 905.
[7] (a) J. Sauer, in: *Modelling of Structure and Reactivity in Zeolites*, ed. C.R.A. Catlow (Academic Press, New York, 1992) p. 183;
(b) J. Sauer, Stud. Surf. Sci. Catal. 84 (1994) 2039.
[8] M. Brändle and J. Sauer, J. Am. Chem. Soc. 120 (1998) 1556.
[9] H.V. Brand, L.A. Curtiss and L.E. Iton, J. Phys. Chem. 97 (1993) 12773.
[10] M.S. Stave and J.B. Nicholas, J. Phys. Chem. 99 (1995) 15046.
[11] R.M. Barrer, *Hydrothermal Chemistry of Zeolites* (Academic Press, London, 1982).
[12] J.B. Uytterhoeven, L.G. Christner and W.K. Hall, J. Phys. Chem. 69 (1965) 2117.
[13] R.A. van Santen and G.J. Kramer, Chem. Rev. 95 (1995) 637.
[14] P.A. Jacobs and J.B. Uytterhoeven, J. Chem. Soc. Faraday Trans. I 69 (1973) 359, 373.
[15] P.A. Jacobs, Catal. Rev.-Sci. Eng. 24 (1982) 415.
[16] E.M. Flanigen, in: *Zeolite Chemistry and Catalyis*, ACS Monograph 171, ed. J.A. Rabo (Am. Chem. Soc., Washington, DC, 1976).
[17] H. Pfeifer, J. Chem. Soc. Faraday Trans. I 84 (1988) 3777.
[18] J. Klinowski, Chem. Rev. 91 (1991) 1459.
[19] D. Fenzke, M. Hunger and H. Pfeifer, J. Magn. Reson. 95 (1991) 477.
[20] E. Brunner, J. Chem. Soc. Faraday Trans. 89 (1993) 165.
[21] P.G. Clarke, K. Gosling, R.K. Harris and E.G. Smith, Zeolites 13 (1993) 388.
[22] G. Engelhardt and D. Michel, *High-Resolution Solid-State NMR of Silicates and Zeolites* (Wiley, Chichester, 1987).
[23] W.P.J.H. Jacobs, J.W. de Haan, L.J.M. van de Ven and R.A. van Santen, J. Phys. Chem. 97 (1993) 10394.
[24] M. Hunger, M.W. Anderson and H. Pfeifer, Microporous Mater. 1 (1993) 17.
[25] L.W. Beck, J.L. White and J.F. Haw, J. Am. Chem. Soc. 116 (1994) 9657.
[26] E. Brunner, Catalysis Today 38 (1997) 361.
[27] J.F. Haw, T. Xu, J.B. Nicholas and P.W. Goguen, Nature 389 (1997) 832.

[28] U. Eichler, M. Brändle and J. Sauer, J. Phys. Chem. 101 (1997) 10035.
[29] R. Car and M. Parinello, Phys. Rev. Lett. 55 (1985) 2471.
[30] G.J. Kramer, A.J.M. de Man and R.A. van Santen, J. Am. Chem. Soc. 113 (1991) 6435.
[31] K.P. Schröder, J. Sauer, M. Leslie, C.R.A. Catlow and J.M. Thomas, Chem. Phys. Lett. 188 (1992) 320.
[32] P. Sarv, T. Tuherm, E. Lippmaa, K. Keskinen and A. Root, J. Phys. Chem. 99 (1995) 13763.
[33] M. Hunger, Solid State NMR 6 (1996) 1.
[34] J. Sauer, M. Sierka and F. Haase, in: *Transition State Modelling of Catalysis in Computational Chemistry*, ACS Symp. Ser., eds. K. Morokuma and D.G. Truklar (ACS, Washington), in press.
[35] T. Baba, N. Komatsu, Y. Ono and H. Sugisawa, J. Phys. Chem. B 102 (1998) 804.
[36] L. Pauling, J. Am. Chem. Soc. 51 (1929) 1010.
[37] (a) S.L. Meisel, J.P. McCullogh, C.H. Lechthaler and P.B. Weisz, CHEMTECH 6 (1976) 86;
(b) C.D. Chang, *Hydrocarbons from Methanol* (Dekker, New York, 1983).
[38] L. Smith, A.K. Cheetham, R.E. Morris, L. Marchese, J.M. Thomas, P.A. Wright and J. Chen, Science 271 (1996) 799.
[39] M. Krossner and J. Sauer, J. Phys. Chem. 100 (1996) 6199.
[40] (a) J. Sauer, Science 271 (1996) 774;
(b) V. Termath, F. Haase, J. Sauer, J. Hutter and M. Parrinello, J. Am. Chem. Soc. 120 (1998) 8512.
[41] M. Bonn, H.J. Bakker, K. Domen, C. Hirose, A.W. Kleyn and R.A van Santen, Catal. Rev., submitted.
[42] R. Shah, J.D. Gale and M.C. Payne, J. Phys. Chem. B 101 (1997) 4787.
[43] E. Nusterer, P.E. Blöchl and K. Schwarz, Chem. Phys. Lett. 253 (1996) 448.
[44] F. Haase, J. Sauer and J. Hutter, Chem. Phys. Lett. 266 (1997) 397.
[45] J. Sauer, P. Ugliengo, E. Garrone and V.R. Saunders, Chem. Rev. 94 (1994) 2095.
[46] G.J. Kramer, R.A. van Santen, C.A. Emeis and A.K. Nowak, Nature 363 (1993) 529.
[47] R.A. van Santen and J.W. Niemantsverdriet, *Chemical Kinetics and Catalysis* (Plenum Press, New York, 1995).
[48] A.G. Pelmenschikov and R.A. van Santen, J. Phys. Chem. 97 (1993) 10678.
[49] H. Ernst, D. Freude, T. Mildner and I. Wolf, Z. Phys. Chem. 189 (1995) 221.
[50] D.B. Ferguson and J.F. Haw, Anal. Chem. 67 (1995) 3342.
[51] E.J. Munson, A.A. Kheir, N.D. Lazo and J.F. Haw, J. Phys. Chem. 96 (1992) 7740.
[52] F. Salehirad and M.W. Anderson, J. Catal. 164 (1996) 301.
[53] J.L. White, L.W. Beck and J.F. Haw, J. Am. Chem. Soc. 114 (1992) 6182.
[54] A.G. Stepanov, A.G. Maryasov, V.N. Romannikov and K.I. Zamaraev, Magn. Reson. Chem. 32 (1994) 16.
[55] R.L. Portsmouth, M.J. Duer and L.F. Gladden, J. Chem. Soc. Faraday Trans. 91 (1995) 559.
[56] V. Bosácek, J. Phys. Chem. 97 (1993) 10732.
[57] L. Reven, J. Molec. Catal. 86 (1994) 447.
[58] A. Seidel and B. Boddenberg, Z. Naturforsch. 50a (1994) 199.
[59] E. Brunner, H. Pfeifer, T. Wutscherk and D. Zscherpel, Z. Phys. Chem. 178 (1992) 173.
[60] C.P. Grey and B.S. Arun Kumar, J. Am. Chem. Soc. 117 (1995) 9071.
[61] L.W. Beck, T. Xu, J.B. Nicholas and J.F. Haw, J. Am. Chem. Soc. 117 (1995) 11594.
[62] M. Koch, E. Brunner, H. Pfeifer and D. Zscherpel, Chem. Phys. Lett. 228 (1994) 501.
[63] H. Klein, H. Fuess and M. Hunger, J. Chem. Soc. Faraday Trans. 91 (1995) 1813.
[64] J.F. Haw, M.B. Hall, A.E. Alvarado-Swaisgood, E. Munson, Z. Lin, L.W. Beck and T. Howard, J. Am. Chem. Soc. 116 (1994) 7308.
[65] J. Jänchen, J.H.M.C. van Wolput, L.J.M. van de Ven, J.W. de Haan and R.A. van Santen, Catal. Lett. 39 (1996) 147.
[66] C. Dybowski, J. Incl. Phenom. Molec. Recogn. Chem. 21 (1995) 113.
[67] W.M. Shirley, C.A. Powers and J.S. Frye, Inorg. Chem. 30 (1991) 4182.
[68] J. Šepa, R.J. Gorte, D. White, E. Kassab and M. Allavena, Chem. Phys. Lett. 262 (1996) 321.
[69] I. Kustanovich, Z. Luz, S. Vega and A.J. Vega, J. Phys. Chem. 94 (1990) 3138.
[70] A. Simon, L. Delmotte, J.M. Chezeau and L. Huve, Chem. Commun. (1997) 263.
[71] V.M. Mastikhin, Coll. Surf. A 78 (1993) 143.
[72] R.J. Gorte and D. White, Topics in Catalysis 4 (1997) 57.
[73] C.T.W. Chu and C.D. Chang, J. Phys. Chem. 89 (1985) 1569.
[74] E.G. Derouane and J.G. Fripiat, J. Phys. Chem. 91 (1987) 145.
[75] P.J. O'Malley and J. Dwyer, Chem. Phys. Lett. 143 (1988) 97.
[76] B. Berglund and R.W. Vaughan, J. Chem. Phys. 73 (1980) 2037.
[77] C.M. Rohlfing, L.C. Allen and R. Ditchfield, J. Chem. Phys. 79 (1983) 4958.
[78] R. Kaliaperumal, R.E.J. Sears, Q.W. Ni and J.E. Furst, J. Chem. Phys. 91 (1989) 7387.
[79] G.A. Jeffrey and Y. Yeon, Acta Crystallogr. B42 (1986) 410.
[80] H. Eckert, J.P. Yesinowski, L.A. Silver and E.M. Stolper, J. Phys. Chem. 92 (1988) 2055.
[81] H. Rosenberger, G. Scheler and Yu.N. Moskvich, Magn. Reson. Chem. 27 (1989) 50.
[82] R.K. Harris, P. Jackson, L.H. Merwin, B.J. Say and G. Hägele, J. Chem. Soc. Faraday Trans. 1 84 (1988) 3649.
[83] U. Sternberg and E. Brunner, J. Magn. Reson. Ser. A 108 (1994) 142.
[84] R. Ditchfield, J. Chem. Phys. 65 (1976) 3123.
[85] M. Catti, G. Ferraris and A. Filhol, Acta Crystallogr. B33 (1977) 1223.
[86] W.R. Busing and H.A. Levy, J. Chem. Phys. 26 (1957) 563.
[87] G. Ferraris and M. Franchini-Angela, Acta Crystallogr. B28 (1972) 2572.
[88] A. Novak, Structure and Bonding 18 (1974) 177.
[89] H.D. Lutz, Structure and Bonding 69 (1988) 97.
[90] H. Koller, Thesis, University of Stuttgart (1993).
[91] R.L. Schmid, J. Felsche and G.J. McIntyre, Acta Crystallogr. C40 (1984) 733.
[92] R.L. Schmid, J. Felsche and G.J. McIntyre, Acta Crystallogr. C41 (1985) 638.
[93] H. Koller, G. Engelhardt and J. Felsche, Z. Anorg. Allg. Chem. 621 (1995) 301.
[94] R. Eckman, J. Chem. Phys. 76 (1982) 2767.
[95] C.I. Ratcliffe, J.A. Ripmeester and J.S. Tse, Chem. Phys. Lett. 120 (1985) 427.
[96] F. Haase and J. Sauer, J. Am. Chem. Soc. 117 (1995) 3780.
[97] S.R. Blaszkowski and R.A. van Santen, J. Phys. Chem. 99 (1995) 11728.
[98] J.D. Gale, C.R.A. Catlow and J.R. Carruthers, Chem. Phys. Lett. 216 (1993) 155.
[99] S. Bates and J. Dwyer, J. Mol. Struct. (THEOCHEM) 306 (1994) 57.
[100] Z. Luz and A.J. Vega, J. Phys. Chem. 91 (1987) 374.
[101] M. Hunger, D. Freude and H. Pfeifer, J. Chem. Soc. Faraday Trans. 87 (1991) 657.
[102] F. Deng, Y. Yue and C. Ye, Solid State NMR 10 (1998) 151.
[103] (a) P. Batamack, C. Dorémieux-Morin, R. Vincent and J. Fraissard, Chem. Phys. Lett. 180 (1991) 545;
(b) P. Batamack, C. Dorémieux-Morin, R. Vincent and J. Fraissard, J. Phys. Chem. 97 (1993) 9779.
[104] G. Mirth, J.A. Lercher, M.W. Anderson and J. Klinowski, J. Chem. Soc. Faraday Trans. 86 (1990) 3039.
[105] M.W. Anderson, P.J. Barrie and J. Klinowski, J. Phys. Chem. 95 (1991) 235.

[106] M. Hunger, T. Horvath, G. Engelhardt and H.G. Karge, Stud. Surf. Sci. Catal. 94 (1995) 756.
[107] M. Hunger and T. Horvath, J. Am. Chem. Soc. 118 (1996) 12302.
[108] F. Haase and J. Sauer, J. Phys. Chem. 98 (1994) 3083.
[109] J. Kotrla, D. Nachtigallová, L. Kubelková, L. Heeribout, C. Doremieux-Morin and J. Fraissard, J. Phys. Chem. B 102 (1998) 2454
[110] J. Seelig, Quarterly Reviews of Biophysics 3 (1977) 353.
[111] R.G. Barnes, Adv. Nucl. Quadrupole Reson. 1 (1974) 335.
[112] K. Schmidt-Rohr and H.W. Spiess, *Multidimensional Solid-State NMR and Polymers* (Academic Press, London, 1994).
[113] M. Hunger and T. Horvath, Ber. Bunsenges. Phys. Chem. 99 (1995) 1316.
[114] A.J. Vega, J. Am. Chem. Soc. 110 (1988) 1049.
[115] J. Šepa, R.J. Gorte, B.H. Suits and D. White, Chem. Phys. Lett. 289 (1998) 281.
[116] J. Šepa and D. White, (1998), personal communication.
[117] H. Ernst, D. Freude and I. Wolf, Chem. Phys. Lett. 212 (1993) 588.
[118] D. Freude and J. Haase, NMR Basic Principles and Progress 29 (1993) 1.
[119] C.P. Grey and A.J. Vega, J. Am. Chem. Soc. 117 (1995) 8232.
[120] A.J. Vega and Z. Luz, J. Phys. Chem. 91 (1987) 365.
[121] D. Fenzke, D. Freude, T. Fröhlich and J. Haase, Chem. Phys. Lett. 111 (1984) 171.
[122] L.C. de Ménorval, W. Buckermann, F. Figueras and F. Fajula, J. Phys. Chem. 100 (1996) 465.
[123] H. Koller, E.L. Meijer and R.A. van Santen, Solid State NMR 9 (1997) 167.
[124] E. Nusterer, P.E. Blöchl and K. Schwarz, Angew. Chem. Int. Ed. Engl. 35 (1996) 175.